Separation Science and Technology
Publication details, including instructions for authors and subscription information:
http://www.informaworld.com/smpp/title~content=t713708471

Separation of Complexed Mercury from Aqueous Wastes Using Self-Assembled Mercaptan on Mesoporous Silica

Shas V. Mattigod[a]; Xiangdong Feng[a]; Glen E. Fryxell[a]; Jun Liu[a]; Meiling Gong[a]
[a] PACIFIC NORTHWEST NATIONAL LABORATORY, RICHLAND, WASHINGTON, USA

Online publication date: 16 August 1999

To cite this Article Mattigod, Shas V. , Feng, Xiangdong , Fryxell, Glen E. , Liu, Jun and Gong, Meiling(1999) 'Separation of Complexed Mercury from Aqueous Wastes Using Self-Assembled Mercaptan on Mesoporous Silica', Separation Science and Technology, 34: 12, 2329 — 2345
To link to this Article: DOI: 10.1081/SS-100100775
URL: http://dx.doi.org/10.1081/SS-100100775

SEPARATION SCIENCE AND TECHNOLOGY, **34**(12), pp. 2329–2345, 1999

Separation of Complexed Mercury from Aqueous Wastes Using Self-Assembled Mercaptan on Mesoporous Silica

SHAS V. MATTIGOD,* XIANGDONG FENG, GLEN E. FRYXELL, JUN LIU, and MEILING GONG
PACIFIC NORTHWEST NATIONAL LABORATORY
RICHLAND, WASHINGTON 99352, USA

ABSTRACT

Separation of Hg(II) from potassium iodide/sulfate wastes was studied using a novel mesoporous silica material containing self-assembled mercaptan groups. The adsorbent, consisting of self-assembled mercaptan on mesoporous silica (SAMMS) developed at Pacific Northwest National Laboratory (PNNL), was characterized as to its specificity, adsorption capacity, and kinetics for separation of mercury from potassium iodide/sulfate solutions. Aqueous speciation calculations indicated that a major fraction (92–99%) of dissolved mercury in the potassium iodide/sulfate wastes solutions existed as HgI_4^{2-} species. The adsorption data showed that the mercury adsorption capacity of SAMMS material increased with decreasing iodide concentrations. The magnitude of calculated free energy of adsorption indicated that mercury adsorption on this adsorbent is typical of soft acid–soft base interactions. High specificity for anionic complexes of Hg(II) by the SAMMS material was confirmed by distribution coefficient measurements. The kinetics data indicated that the adsorption reactions occur very rapidly independent of Hg(II) concentrations and pH. These tests confirmed that SAMMS material can very effectively remove strongly complexed Hg(II) from aqueous wastes.

Key Words. Mercury removal; Mercury adsorption; Mercury speciation; Mesoporous silica

* To whom correspondence should be addressed. FAX: (509) 376-5368. E-mail: shas.mattigod@pnl.gov

INTRODUCTION

The activities of the US Department of Energy (DOE) over a period of decades have resulted in a large volume (about 50,000 m^3) of mercury containing mixed low-level and transuranic wastes. These Hg-bearing DOE wastes consist of aqueous and nonaqueous liquids, sludges, soils, absorbed liquids, partially or fully stabilized sludges, and debris. So far, no effective treatment technology has been developed for removing the Hg contained in these wastes (1).

One of the technologies being tested involves mobilizing mercury from solid wastes using a lixiviant consisting of an aqueous solution of potassium iodide/iodine (2). This patented process utilizes solutions consisting of I_2 (0.001 to 0.5 M) as the oxidizing agent and the iodide ion (from 0.1 to 1.0 M) as a complexing ligand. Mercury in contaminated solid wastes in the form of oxides, sulfides, elemental, solid:solution phases, and as adsorbed phases is mobilized by the KI/I_2 lixiviant through oxidation and complex formation reactions. After such mobilization, the dissolved and strongly complexed Hg must be removed before the lixiviant is recycled.

For this purpose, a novel adsorber material consisting of self-assembled mercaptan groups on mesoporous silica (SAMMS) substrate has been developed at PNNL (3). This adsorbent has specifically designed functional groups that have very high specificity and adsorption capacity for Hg and other soft cationic contaminants of concern. The pores in SAMMS have a very narrow, specifically tailored (15 to 400 Å) pore-size distribution, resulting in a very high surface area (>800 m^2/g).

The SAMMS adsorbent is synthesized by utilizing the principle of molecular self-assembly in which functional molecules are induced to aggregate on an active surface, resulting in an organized assembly with both order and orientation (3–6). During this process, bifunctional molecules containing hydrophilic and hydrophobic moities adsorb onto an engineered substrate or interface as closely packed monolayers. Such a self-assembly of functional molecules is driven by both inter- and intramolecular forces. The hydrophobic and hydrophilic moities of these functional molecules can be chemically modified to contain specific functional groups to promote covalent bonding between the functional organic molecules and the substrate on one end and molecular bonding between organic molecules and the metallic ions on the other end. By populating the outer surface with an optimum density of functional groups, an effective means for specifically binding certain metal ions can be established. The metal-loading capacity of such an assemblage is determined by the functional group density that, in turn, is controlled by the available surface area of the underlying inorganic engineered substrate.

The objective of this study is to demonstrate the effectiveness of the SAMMS adsorber in removing strongly complexed Hg(II) from spent KI lix-

iviant. The scope of our study included the investigation of kinetics, loading capacity, and distribution coefficient for Hg adsorption on SAMMS material. The parameters investigated included ionic strengths, iodide concentrations, pH conditions, and soluble Hg concentrations.

EXPERIMENTAL

Materials and Method

Preparation of SAMMS Adsorber Material

The SAMMS adsorber used in these investigations was synthesized through a coassembly process using oxide precursors and surfactant molecules (3, 7–11). The synthetic process consisted of mixing surfactants and oxide precursors in a solvent and reacting the resulting solution under mild hydrothermal conditions. The process consisted of forming ordered liquid-crystalline structures, such as hexagonally ordered rodlike micelles, by the surfactant molecules, then precipitating oxide materials on the micellar surfaces to replicate the organic templates formed by the rodlike micelles. Calcination of the organic-oxide micelle structures at 500°C removed the surfactant templates, resulting in a high surface area mesoporous oxide structure. Functionalized monolayers, consisting of thiol groups, were formed on the pore surfaces of the mesoporous oxide structure using tris-(methoxy)mercaptopropylsilane in an appropriate solvent (3). These thiol functional groups are known to have very high specificity for binding soft cations such as Hg. The SAMMS material used in our investigations consisted of particles 5 to 15 μm in size with pore sizes of 5 nm and 871 m^2/g of surface area. The thiol group density was measured to be about 2.8 mmol/g of SAMMS. Preliminary tests showed that approximately 2.5 mmol of Hg could be loaded per gram of this material, indicating that about 90% of the thiol groups in SAMMS are accessible for metal adsorption (3). Additional tests of this SAMMS material also indicated a high binding affinity for Hg ($K_d \approx 1 \times 10^8$ mL/g) (3).

Aqueous Speciation of Mercury

The adsorption of Hg is influenced by the types and concentrations of aqueous species of Hg and other competing dissolved species that are present in the waste solutions. To help interpret the adsorption data, the aqueous speciation of Hg in different matrix solutions (Tables 2 and 3) was calculated using the equilibrium code GEOCHEM (12–14). The input data for the speciation calculations consisted of the total concentrations of metals [K, Ca, Fe(II), and Hg], ligands (iodide and sulfate), and measured pH (5.0–5.5) for each solution. The output from these calculations consisted of true ionic strength, and the concentrations and activities of both free and complexed species. The as-

TABLE 1
Stability Constants and Solubility Product Constants Used in Speciation Calculations

Reaction	log *K*	Source
Aqueous Species		
$Hg^{2+} + NO_3^- = HgNO_3^+$	0.77	15
$Hg^{2+} + 2NO_3^- = Hg(NO_3)_2^0$	1.00	15
$Hg^{2+} + OH^- + NO_3^- = HgOHNO_3^0$	11.70	18
$Hg^{2+} + OH^- = HgOH^+$	10.60	15
$Hg^{2+} + 2OH^- = Hg(OH)_2^0$	21.80	15
$Hg^{2+} + 3OH^- = Hg(OH)_3^-$	20.90	15
$2Hg^{2+} + OH^- = Hg_2OH^{3+}$	10.70	15
$3Hg^{2+} + 3OH^- = Hg_3(OH)_3^{3+}$	35.60	15
$Hg^{2+} + I^- = HgI^+$	13.41	15
$Hg^{2+} + 2I^- = HgI_2^0$	24.68	15
$Hg^{2+} + 3I^- = HgI_3^-$	28.41	15
$Hg^{2+} + 4I^- = HgI_4^{2-}$	30.30	15
$Hg^{2+} + OH^- + I^- = HgOHI^0$	23.46	15
$Hg^{2+} + SO_4^{2-} = HgSO_4^0$	2.50	15
$Hg^{2+} + 2SO_4^{2-} = Hg(SO_4)_2^{2-}$	3.48	15
$Hg^{2+} + HSO_4^- = HgHSO_4^+$	1.10	19
$Hg^{2+} + OH^- + SO_4^{2-} = HgOHSO_4^-$	12.94	18
$Ca^{2+} + NO_3^- = CaNO_3^+$	0.50	17
$Ca^{2+} + 2NO_3^- = Ca(NO_3)_2^0$	0.60	15
$Ca^{2+} + I^- = CaI^+$	0.07	19[a]
$Ca^{2+} + OH^- = CaOH^+$	1.30	15
$Ca^{2+} + 2OH^- = Ca(OH)_2^0$	0.00	21
$Ca^{2+} + SO_4^{2-} = CaSO_4^0$	2.30	17
$Fe^{2+} + OH^- = FeOH^+$	4.70	16
$Fe^{2+} + 2OH^- = Fe(OH)_2^0$	7.40	16
$Fe^{2+} + 3OH^- = Fe(OH)_3^-$	9.30	16
$Fe^{2+} + 4OH^- = Fe(OH)_4^{2-}$	8.90	16
$Fe^{2+} + SO_4^{2-} = FeSO_4^0$	2.20	15
$Fe^{2+} + 2SO_4^{2-} = Fe(SO_4)_2^{2-}$	0.76	15
$Fe^{2+} + HSO_4^- = FeHSO_4^-$	1.08	22
$Fe^{2+} + NO_3^- = FeNO_3^+$	0.30	22
$Fe^{2+} + I^- = FeI^+$	3.67	19[a]
$Fe^{2+} + 2I^- = FeI_2^0$	5.80	19[a]
$Fe^{2+} + OH^- + I^- = FeOHI^0$	6.90	18
$K^+ + NO_3^- = KNO_3^0$	−0.19	17
$K^+ + I^- = KI^0$	−0.19	15
$K^+ + SO_4^{2-} = KSO_4^-$	0.85	17
$K^+ + OH^- = KOH^0$	−0.50	15
$H^+ + SO_4^{2-} = HSO_4^-$	1.99	15
$H^+ + OH^- = H_2O$	14.00	15

MARCEL DEKKER, INC.
270 Madison Avenue, New York, New York 10016

TABLE 1 Continued

Reaction	log K_{sp}	Source
Solid Phases		
$Hg^{2+} + 2OH^- = H_2O + HgO(s)$	25.44	15
$Hg^{2+} + SO_4^{2-} = HgSO_4(s)$	3.30	20[b]
$Ca^{2+} + 2OH^- = Ca(OH)_2(s)$	5.19	15
$Ca^{2+} + SO_4^{2-} + 2H_2O = CaSO_4 \cdot 2H_2O(s)$	4.62	16
$Fe^{2+} + 2OH^- = Fe(OH)_2(s)$	14.40	15

[a] Estimated using the method of Nieber and McBryde in Ref. 19.

sociation constants for aqueous complexes and the solubility product constants of solid phases used in the computations are listed in Table 1.

Adsorption Density Experiments

The objective of these experiments was to measure the range of Hg adsorption on SAMMS material that can be achieved from matrix solutions formulated as surrogates for leachates from actual Hg-containing wastes. The compositions of surrogate solutions were developed based on the composition of the actual leachate solutions resulting from KI/I_2 lixiviant solutions. According to the actual leachate data, the dominant dissolved constituents in the actual Hg-containing waste streams are K^+, I^-, and I_2, with minor amounts of Fe^{2+} and SO_4^{2-}. Based on this information, a series of surrogate solutions was prepared containing varying concentrations of I, K, Hg, and other minor constituents. These solutions were formulated to represent varying compositions of leachates, washwaters, and combinations of these waste streams. The Hg concentrations used in these experiments ranged from ~0.5 to 2.9 mmol/L.

Generally, the contaminant loading on an exchange material is affected by several factors such as the composition of the matrix solution (competing ions, ionic strength, and pH), concentration of contaminant, solid:solution ratio, and contact time. In this set of experiments the effects of KI concentrations and solid:solution ratios were tested with a fixed contact time of 4 hours. The compositions of the surrogate test solutions used in these experiments are listed in Table 2. The loading experiments were conducted in duplicate (except two very high solid:solution ratio experiments), with surrogate solutions and varying quantities of SAMMS material to achieve ratios ranging from 1:200 to 1:4000. The surrogate solutions were contacted with SAMMS material for 4 hours to achieve equilibrium. Following equilibrium, the solutions

MARCEL DEKKER, INC.
270 Madison Avenue, New York, New York 10016

TABLE 2
Matrix Solutions Used in Mercury-Loading Experiments

	Solutions (mmol/L)				
Constituent	S1	S2	S3	S4	S5
Iodide	606	410	350	250	90
Sulfate	20	23	54	54	88
K	635	440	450	350	265
Fe(II)	3	3	2	2	0.5
Ca	—	—	0.1	0.1	0.2
Hg	2.34	2.89	1.30	1.69	0.49

were separated from the SAMMS material using 0.2-μm syringe filters. The Hg concentrations in the equilibrated solutions were determined by cold vapor atomic adsorption spectroscopy (CVAA).

Distribution Coefficient Measurements

Distribution coefficient is the measure of an exchange substrate's selectivity or specificity for adsorbing a specific contaminant or a group of contaminants from matrix solutions, such as waste streams. The distribution coefficient (sometimes referred to as the partition coefficient at equilibrium) is defined as a ratio of the adsorption density to the final contaminant concentration in solution at equilibrium. This measure of selectivity is defined as $K_d = A_{eq}/C_{eq}$, where K_d is the distribution coefficient (mL/g), A_{eq} is the equilibrium adsorption density (mg of contaminant per gram of adsorbing substrate), and C_{eq} is the contaminant concentration (mg/mL) in contacting solution at equilibrium. The partition coefficient is defined as $K_p = A/C$, where K_p is the partition coefficient (mL/g), A is the adsorption density (mg of contaminant per gram of adsorbing substrate) at any stage before equilibrium is attained, and C is the contaminant concentration (mg/mL) in contacting solution at the same stage as the adsorption is calculated. At equilibrium, K_p will be equal to K_d.

The K_ds were measured by equilibrating 25- and 100-mg quantities of SAMMS material with 20 mL of contact solution (solid:solution ratios of 1:800 and 1:200, respectively). The contact solutions were formulated with two different Hg concentrations (~0.3 and ~0.5 mmol/L). The concentrations of major constituents in both solutions consisted of ~270 mmol of potassium, ~90 mmol/L of iodide, ~90 mmol/L of sulfate, and minor concentrations of Fe(II) and calcium. The solution compositions used in these experiments are listed in Table 3. Following 4 hours of equilibration, the aliquots of equili-

MARCEL DEKKER, INC.
270 Madison Avenue, New York, New York 10016

TABLE 3
Experimental Conditions Used for
Measuring the Distribution Coefficients

	Solution (mmol/L)	
Constituent	K1	K2
Iodide	90	90
Sulfate	88	88
K	265	265
Fe(II)	0.5	0.5
Ca	0.2	0.2
Hg	0.33	0.49

brated solutions were filtered through a 0.2-μm filter and Hg concentrations were measured by CVAA.

Kinetics Experiments

A set of experiments was designed to study the kinetics of adsorption of dissolved Hg from a matrix solution of 100 mmol/L KI. The binding kinetics were assessed using batch adsorption experiments at four different pH values (3, 5, 7, and 9). The rates of adsorption were monitored by measuring the Hg concentration in the solution phase at selected periodic intervals. Because the rate of adsorption is affected by the initial concentration of adsorbate, two sets of kinetic experiments at each pH value were conducted to examine this phenomenon. The initial Hg concentrations in these experiments were set at ~0.5 and ~1.8 mmol/L, respectively. These concentrations were selected on the basis that this range of Hg concentration may represent the higher range found in KI solution following extraction of actual Hg-bearing wastes. A fixed solid:solution ratio of 1:800 was used in all experiments. The test matrix for the adsorption kinetic studies consisted of eight solutions (two Hg concentrations and four pH values) with seven contact time measurements (0, 5, 10, 30, 60, 120, 180, and 360 minutes).

RESULTS AND DISCUSSION

Predicted Aqueous Speciation of Mercury

The speciation calculations showed that about 92 to 99% of the total dissolved Hg in equilibrium solutions existed as HgI_4^{2-} species (Table 4). The remaining fraction of the dissolved Hg was predicted to be in the form of HgI_3^- species (from 1 to 8%). In these solutions, no solid precipitation reactions were predicted to occur, thus Hg in these systems would occur only in dis-

TABLE 4
Computed Speciation (%) of Soluble Constituents in the Equilibrium Solutions

		Equilibrating solution				
Component	Species	S1	S2	S3	S4	S5
Hg	HgI_4^{2-}	98.9	98.2	97.7	97.1	92.3
	HgI_3^-	1.1	1.2	2.3	2.9	7.7
K	K^+	87.0	88.0	86.6	88.0	87.2
	KI^0	11.6	9.7	8.2	6.2	2.3
	KSO_4^-	1.4	2.3	5.2	5.8	10.5
Ca	Ca^{2+}	81.8	76.5	65.0	63.4	50.8
	CaI^+	10.9	8.8	6.6	4.6	1.4
	$CaSO_4^0$	7.3	14.7	28.4	32.0	47.8
Fe	FeI_2^0	96.5	95.9	95.3	93.8	84.5
	FeI^+	3.5	4.1	4.7	6.2	15.3

solved and adsorbed forms. Further, the Hg speciation indicates that adsorption reactions would be controlled by the concentration (activity) of the dominant form, namely mercury iodide complex (HgI_4^{2-}) species. The speciation of other dissolved constituents such as K, Ca, and Fe are also listed in Table 4.

Adsorption Density Measurements

The data show that the adsorption density of Hg on SAMMS can range from 26 to 270 mg/g, depending on the composition of matrix solution and solid:solution ratio (Table 5). Because HgI_4^{2-} was predicted to be the dominant aqueous species of Hg in these solutions, the adsorption mechanism may consist of dissociation of HgI_4^{2-} species followed by adsorption of the free form of the metal on to thiol groups as follows:

$$HgI_4^{2-} = Hg^{2+} + 4I^- \quad (1)$$

$$\text{SAMMS-R(SH)}_2 + Hg^{2+} = \text{SAMMS-RS}_2\text{Hg} + 2H^+ \quad (2)$$

The overall reaction for the adsorption of complexed Hg can be expressed as the sum of Reactions (1) and (2):

$$\text{SAMMS-R(SH)}_2 + HgI_4^{2-} = \text{SAMMS-RS}_2\text{Hg} + 4I^- + 2H^+ \quad (3)$$

The adsorption data (Table 5) also indicate that at a fixed solid:solution ratio with sufficient Hg to saturate the adsorption sites, the adsorption density increases with decreasing iodide concentrations. At both solid:solution ratios (1:200 and 1:800), ~40% reduction in iodide concentrations resulted in ~50% increase in Hg adsorption by SAMMS. Such an increase in adsorption with decreasing iodide concentrations suggests that iodide influences Hg adsorp-

MARCEL DEKKER, INC.
270 Madison Avenue, New York, New York 10016

TABLE 5
Mercury-Loading Data on SAMMS Obtained in Surrogate Solutions Containing Iodide Ions

Solution	Replicate	Solid : solution ratio	I concentration (mmol/L)	Equilibrium Hg concentration (mmol/L)	Hg loading (mg/g)
S1	1	1 : 200	606	1.695	26
S1	2	1 : 200	606	1.645	28
S2	1	1 : 800	410	2.393	78
S2	2	1 : 800	410	2.443	70
S3	1	1 : 200	350	0.273	41
S3	2	1 : 200	350	0.276	41
S4	1	1 : 800	250	1.047	105
S4	2	1 : 800	250	0.997	113
S4	1	1 : 4000	250	1.496	165
S5	1	1 : 800	90	0.003	77
S5	2	1 : 800	90	0.002	84
S5	1	1 : 4000	90	0.150	270

tion through complex formation. A fivefold change in solid:solution ratio (1:800 to 1:4000) at a fixed iodide and initial Hg concentration resulted in a ~50% increase in Hg adsorption by SAMMS, indicating that increasing the solid:solution ratios also increases Hg adsorption. The highest Hg adsorption density of 270 mg/g of SAMMS was observed when I concentration in the matrix solution was 90 mmol/L at a solid:solution ratio of 1:4000.

These Hg adsorption density data may be compared to previous data (23) obtained in matrix solutions consisting of 100 mmol/L $NaNO_3$ with initial Hg concentrations ranging from 0.00024 to 670 mg/L. Adsorption densities of 83 to 635 mg/g observed in previous experiments indicate that $NaNO_3$ medium do not influence Hg adsorption on SAMMS to the same extent that the KI–K_2SO_4 medium do in these experiments. Data obtained in previous and current studies under somewhat similar experimental conditions (solid:solution ratio and initial Hg concentration) show that in KI–K_2SO_4 medium the adsorption density achieved is about one-half of the adsorption density attained in $NaNO_3$ matrix solution (Table 6). Calculated speciation indicate that

TABLE 6
Comparison of Mercury-Loading Data Obtained in Nitrate and Iodide Matrix Solutions

Matrix solution	Hg concentration (mmol/L)	Solid : solution ratio	Hg adsorbed (mg/g)	Source
KI	0.489	1 : 4000	270	This study
$NaNO_3$	0.563	1 : 5000	415	23

in $NaNO_3$ media, dissolved Hg exists in the form of Hg^{2+} (37%), $Hg(OH)_2^0$ (30%), $HgOH^+$ (14%), $HgOHNO_3^0$ (10%), and $HgNO_3^+$ (9%). By comparison, in KI–K_2SO_4 medium, in comparison, dissolved Hg exists as HgI_4^{2-} (92%) and HgI_3^- (8%). These data comparisons suggest that anionic Hg–I complexes are adsorbed to a lesser extent by SAMMS than the free (uncomplexed), cationic, and neutral complexes of Hg. These data clearly indicate that Hg speciation in solution significantly influences the extent of adsorption on SAMMS material.

Free Energy of Adsorption

The speciation calculations showed that the HgI_4^{2-} species was the dominant form (from 92 to 99%) of the total dissolved Hg. Therefore, adsorption of dissolved Hg on SAMMS material may occur through dissociation of HgI_4^{2-} species followed by adsorption onto thiol groups as indicated earlier by Eqs. (1), (2), and (3). The equilibrium constants as a function of activities of reactants and products in the above reactions are expressed as:

$$K_1 = (Hg^{2+})(I)^4/(HgI_4^{2-}) \quad (4)$$

$$K_2 = (-RS_2Hg)(H)^2/(-RSH)^2(Hg^{2+}) \quad (5)$$

$$K_3 = (-RS_2Hg)(H)^2(I)^4/(-RSH)^2(HgI_4^{2-}) \quad (6)$$

The equilibrium constant, K_3, can be evaluated using the computed activities of HgI_4^{2-} and free ionic I species, the measured pH, and calculated adsorbed-phase activity of Hg (calculated as equivalent to mole fraction adsorbed). Equation (6) can be solved graphically using a linearized form as

$$\log K_3 = \log(N_{Hg}) - 2pH + 4\log(I^-) - 2\log(N_H) + \log(HgI_4^{2-}) \quad (7)$$

Rearranging Eq. (7) results in

$$Y = -4\log(I^-) + \log K_3 \quad (8)$$

where

$$Y = \log(N_{Hg}) - 2pH - 2\log(N_H) + \log(HgI_4^{2-})$$

A plot of Y as the dependent and $\log(I^-)$ as the independent variable would yield a slope of -4 and an intercept equal to $\log K_3$. Plotting adsorption data yielded a line with a slope of -3.8 and an intercept of -11.45 (Fig. 1). Using the value of $\log K_3$ (-11.45) and the value of $\log K_1$ (-30.3 from Table 1), the value $\log K_2$ was calculated as

$$\log K_2 = \log K_3 - \log K_1 = -11.45 - (-30.3) = 18.85 \quad (9)$$

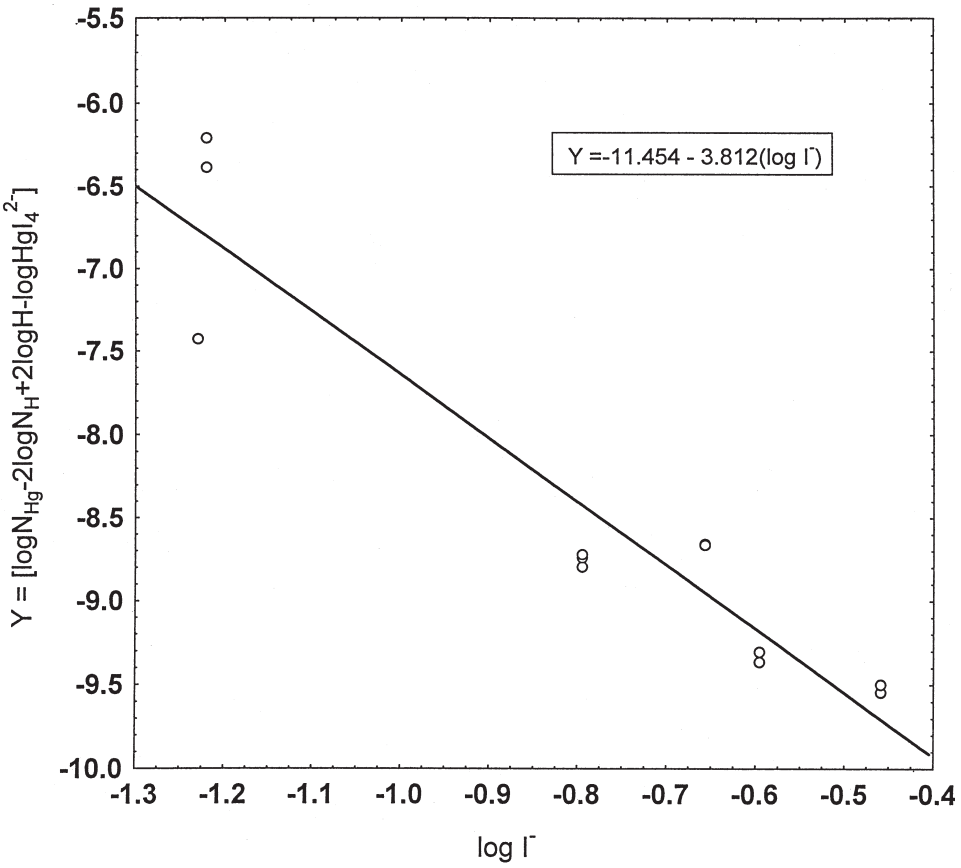

FIG. 1 Mercury adsorption on SAMMS as a function of uncomplexed iodide ion activity.

From this log K_2 value, the free energy of exchange for the reaction

$$\text{SAMMS-R(SH)}_2 + \text{Hg}^{2+} = \text{SAMMS-RS}_2\text{Hg} + 2\text{H}^+ \qquad (10)$$

was calculated to be -107.6 kJ/mol of Hg^{2+}. This value indicates a significantly higher affinity by Hg^{2+} for the thiol groups as compared with divalent metal affinity for silanol groups (-60 kJ/mol, Ref. 24). These differences in adsorption affinity can be explained on the basis of the hard and soft acid base principle (25), which predicts stronger interaction of a soft cation (Hg^{2+}) with a soft base (—SH groups) as compared to the soft cation affinity for silanol groups.

Distribution Coefficient Measurements

The results show that SAMMS material has very high selectivity (very high K_d values) for Hg in iodide-containing surrogate solutions (Table 7). The speciation calculations indicated that in both solutions, HgI_4^{2-} species constituted about 92% of the total dissolved Hg whereas HgI_3^- species formed a minor

TABLE 7
Distribution Coefficients for Adsorption of Mercury by SAMMS Material from Surrogate Solutions

Replicate	Initial Hg concentration (mg/L)	Final Hg concentration (mg/L)	Solid : solution ratio (g/mL)	K_d (mL/g)
K1–1	66	$<5 \times 10^{-5}$	1 : 200	$>2.64 \times 10^8$
K1–2	66	$<5 \times 10^{-5}$	1 : 200	$>2.64 \times 10^8$
K2–1	97.5	0.6	1 : 800	1.29×10^5
K2–2	97.5	0.4	1 : 800	2.10×10^5

fraction (8%). When solutions containing 0.33 mmol/L of total Hg were contacted with SAMMS material, the equilibrium concentrations of Hg were below detection ($<5 \times 10^{-5}$ mg/L using CVAA). Consequently, the calculations show that SAMMS material has extremely high specificity ($K_d > 2.64 \times 10^8$ mL/g) for dissolved Hg (in HgI_4^{2-} and HgI_3^- complex forms) in the tested surrogate solution. The second set of duplicate experiments with solutions containing 0.49 mmol/L of Hg also showed that SAMMS material has very high specificities (K_d of 1.29×10^5 and 2.10×10^5 mL/g) for adsorbing anionic Hg–I complex species. The data obtained from these experiments indicate that SAMMS material, due to its very high selectivity (very high K_d and very low equilibrium Hg concentrations), can be used to remove strongly complexed Hg(II) from KI–K_2SO_4 waste stream solutions with extremely low ($<$0.5 mg/L) residual levels.

Kinetics of Adsorption

The results of the kinetics experiments are shown in Fig. 2. The speciation calculations indicated that dissolved Hg existed mainly as anionic iodide complexes (~92% as HgI_4^{2-} and ~8% as HgI_3^-). The data show that at initial Hg concentrations of ~0.5 mmol/L and at all pH values, ~95% of the final adsorption occurs within the first 5 minutes (Fig. 2). In all cases, adsorption equilibrium seems to have been attained in ~6 hours. In experiments with higher initial concentrations of Hg (~1.8 mmol/L), ~80–85% final adsorption occurred within the first 5 minutes (Fig. 2). Also in this set of experiments, adsorption equilibrium seems to have been attained in ~6 hours.

The kinetics of adsorption on silicate substrates is typically described using either a first- or second-order rate equation (26). The kinetics data obtained in our experiments, however, did not fit either rate equation, indicating that the kinetics of adsorption was not a simple function of the mercury concentration in solution or on the characteristics of the adsorber material. Therefore, the

MARCEL DEKKER, INC.
270 Madison Avenue, New York, New York 10016

data were examined using a simpler functional relationship described by Ungarisch and Aharoni (27). The linearized form of this equation is

$$\ln q = \ln k + (1/\nu) \ln t \tag{11}$$

where q is the amount adsorbed at time, t, and k and ν are constants. The data fit using this equation is shown in Fig. 3, and the constants obtained from the intercept and slope determinations are listed in Table 8.

The kinetics data (Table 8) indicated that at lower initial Hg concentrations (~0.5 mmol/L) there were no significant differences in the rate of adsorption pH values of 5, 7, and 9, whereas at pH 3 the rate appeared to be lower than that observed at higher pH values. This lower rate at pH 3 can be explained on the basis of the proton concentration being higher than the concentration of Hg, thus affecting the rate of proton displacement from thiol groups. As expected, at higher initial Hg concentrations (~1.8 mmol/L), the rate of adsorption is higher and no significant rate difference exists for adsorption at pH values of 3, 5, and 7. However, at pH 9 the observed rate of adsorption is noticeably higher than at lower pH values. Because there are no significant

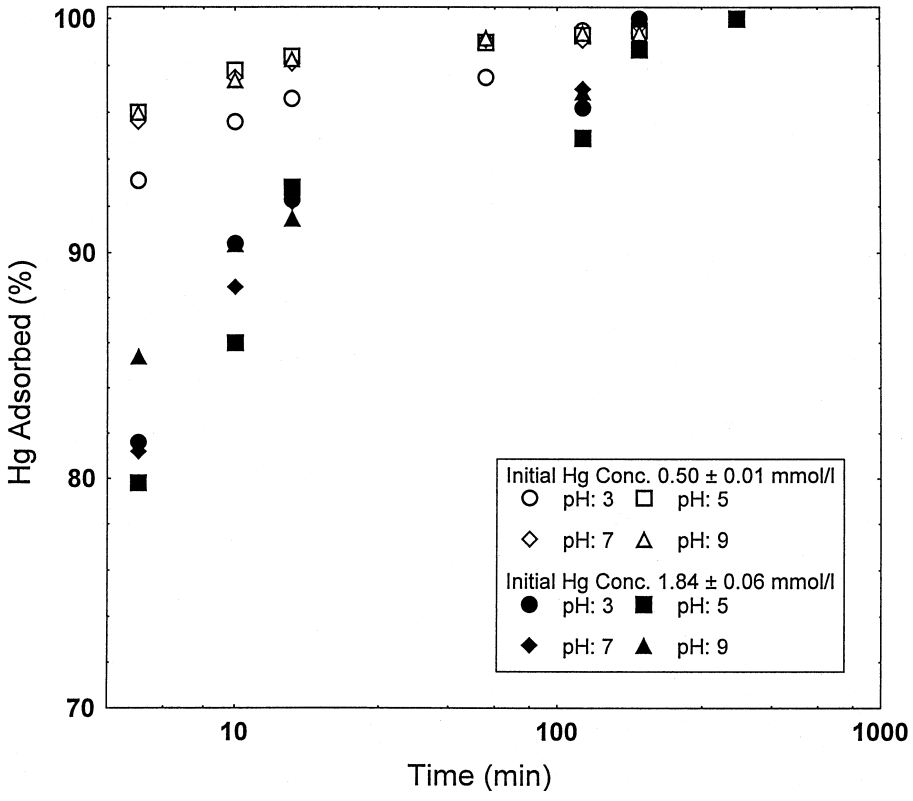

FIG. 2 Kinetics data for mercury adsorption on SAMMS as related to initial mercury concentrations and pH values.

MARCEL DEKKER, INC.
270 Madison Avenue, New York, New York 10016

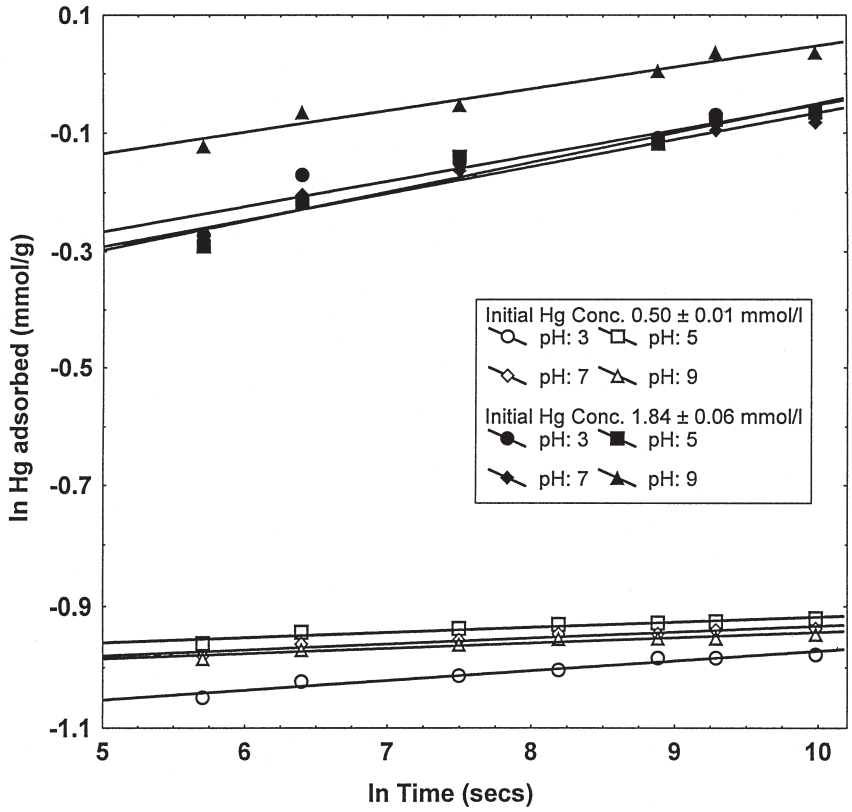

FIG. 3 Linearized functional relationship for kinetics of mercury adsorption on SAMMS.

differences in Hg speciation (the dominant species at all pH values was predicted to be HgI_4^{2-}), the higher rate of adsorption at pH 9 could be attributed to the higher proportion of dissociated thiol groups (log dissociation constant of thiol groups is approximately −9.3) at this pH. Thus, the higher rate of ad-

TABLE 8
Kinetics Data for Mercury Binding by SAMMS Material

Initial Hg concentration (mmol/L)	pH	k (mmol·g^{-1}·s^{-1})	v	r^2
0.51	3	0.321	61.5	0.950
0.51	5	0.367	118.3	0.914
0.50	7	0.357	102.3	0.915
0.50	9	0.357	114.2	0.925
1.87	3	0.619	23.4	0.891
1.78	5	0.580	20.2	0.934
1.78	7	0.596	22.2	0.935
1.90	9	0.729	27.5	0.954

sorption can be attributed to the higher affinity of dissociated thiol groups for dissolved Hg species as compared to undissociated thiol groups.

The rapid rates of Hg adsorption onto SAMMS materials observed in these experiments are similar to the reaction rates observed previously (23) for adsorption on SAMMS in 0.1 M $NaNO_3$ solutions with very low initial concentrations of Hg (0.5 and 10 mg/L). In $NaNO_3$ medium, the speciation calculations show that the dissolved Hg exists mainly in the form of neutral hydrolytic species [$Hg(OH)_2^0$]. These calculations show that the dissolved Hg is adsorbed at a relatively high rate irrespective of the concentration, type, and charge of Hg complex species [HgI_4^{2-} or $Hg(OH)_2^0$] in waste solution.

CONCLUSIONS

- The adsorption density measurements indicate that SAMMS material can adsorb from 26 to 270 mg/g of strongly complexed Hg (as HgI422) from potassium iodide/sulfate waste solutions. The adsorption density increased with decreasing iodide concentration.
- Dissolved Hg(II) has a higher affinity for thiol groups in SAMMS as compared to silanol groups in silica gel, affirming the nature of soft cation–soft base interaction expected between Hg and -SH groups.
- The distribution coefficient data showed that SAMMS can be used effectively to remove strongly complexed Hg(II) from waste solutions.
- Kinetic studies indicated that SAMMS material adsorbs anionic Hg(II) complexes at a relatively rapid rate irrespective of the concentration and pH of waste solutions.

ACKNOWLEDGMENTS

This study was supported by the Mixed Waste Focus Area, Office of Science and Technology of the US Department of Energy. Pacific Northwest National Laboratory is operated for the US Department of Energy by Battelle under Contract DE-AC06-76RLO 1830. We thank Thomas Klasson of Oak Ridge National Laboratory for providing waste solution data, Dan Kaplan for technical review, and R. Schrempf for editorial review.

REFERENCES

1. INEL, *Mercury Removal/Extraction* (INEL/EXT-97-00317, LMITCO Controlled Document, Rev 0), Lockheed Martin, Idaho Falls, ID, 1997. http://wastenot.inel.gov/mwfa/tdrd.html
2. D. F. Foust, "Extraction of Mercury and Mercury Compounds from Contaminated Material and Solutions." US Patent 5,226,545 (1993).
3. X. Feng, G. E. Fryxell, L. Wang, A. Y. Kim, J. Liu, and K. M. Kemner. "Functionalized Monolayers on Ordered Mesoporous Supports," *Science*, *276*, 923–926 (1997).

4. G. E. Fryxell, P. C. Rieke, L. L. Wood, M. H. Engelhard, R. E. Williford, G. L. Graff, A. A. Campbell, R. J. Wiacek, L. Lee, and A. Halverson. "Nucleophilic Displacements in Mixed Self-Assembled Monolayers," *Langmuir*, *11*, 318–326 (1996).
5. B. C. Bunker, P. C. Rieke, B. J. Tarasevitch, A. A. Campbell, G. E. Fryxell, G. L. Graff, L. Song, J. Liu, and J. W. Virden, "Ceramic Thin Film Formation on Functionalist Interfaces through Biomimetic Processing," *Science*, *264*, 48–55 (1994).
6. B. J. Tarasevitch, P. C. Rieke, and J. Liu. "Nucleation and Growth of Oriented Films onto Organic Interfaces," *Chem. Mater.*, *8*, 292–300 (1996).
7. C. T. Kresge, M. E. Leonowicz, W. J. Roth, J. C. Vartuli, and J. S. Beck. "Ordered Mesoporous Molecular Sieves Synthesized by a Liquid Crystal Template Mechanism," *Nature*, *359*, 710–712 (1992).
8. J. S. Beck, J. C. Vartuli, W. J. Roth, M. E. Leonowicz, C. T. Kresge, K. D. Schimitt, C. T. W. Chu, D. H. Olson, E. W. Sheppard, S. B. McCullen, J. B. Higgins, and J. L. Schlenker. "A New Family of Mesoporous Molecular Sieves Prepared with Liquid Crystal Templates," *J. Am. Chem. Soc.*, *114*, 10834 (1992).
9. J. D. LeGrange, J. L. Markham, and C. R. Kurkjian. "Effects of Surface Hydration on the Deposition of Silane Monolayers on Silica," *Langmuir*, 9, 1749–1753 (1993).
10. J. Liu, A. Y. Kim, J. Virden, and B. C. Bunker. "Preparation of Mesoporous Spherulite in Surfactant Solutions," *J. Porous Mater.*, *2*, 201–205 (1995).
11. J. Liu, A. Y. Kim, J. Virden, and B. C. Bunker. "Effect of Colloidal Particles on the Formation of Ordered Mesoporous Materials," *Langmuir*, *11*, 689–692 (1996).
12. S. V. Mattigod and G. Sposito, "Chemical Modeling of Trace Metal Equilibria in Contaminated Soil Solutions Using the Computer Program GEOCHEM," in *Chemical Modeling in Aqueous Systems* (E. A. Jenne, Ed., ACS Symp. Ser. 93), American Chemical Society, Washington, DC, 1979.
13. S. V. Mattigod, "Validation of Geochemical Equilibrium Models," in *Chemical Equilibrium and Reaction Models*, Soil Science Society of America, Madison, WI, 1996.
14. S. V. Mattigod and J. M. Zachara, "Equilibrium Modeling in Soil Chemistry," in *Methods of Soil Analysis*, *Part 3*, *Chemical Methods*, Soil Science Society of America, Madison, WI, 1997.
15. R. N. Smith and A. E. Martell, *Critical Stability Constants*, *V4*, Plenum Press, New York NY, 1976.
16. A. E. Martell and R. N. Smith, *Critical Stability Constants*, *V5*, *I Supplement*, Plenum Press, New York, NY, 1982.
17. R. N. Smith and A. E. Martell, *Critical Stability Constants*, *V6*, *II Supplement*, Plenum Press, New York, NY, 1989.
18. D. Dyrssen, D. Jagner, and F. Wengelin, *Computer Calculation of Ionic Equilibria and Titration Procedures*, Almquist and Wiksell, Stockholm, 1968.
19. E. Nieboer and A. E. McBryde, "Free-Energy Relationships in Coordination Chemistry. III. A Comprehensive Index to Complex Stability," *Can. J. Chem.*, *51*, 2512–2524 (1973).
20. D. D. Wagman, W. H. Evans, V. B. Parker, I. Halow S. M. Bailey, and H. Schumm, *Selected Values of Chemical Thermodynamic Properties*, National Bureau of Standards Technical Notes 270-5, 1969.
21. S. A. Greenberg and L. E. Copeland, "The Thermodynamic Functions for the Solution of Calcium Hydroxide in Water," *J. Phy. Chem.*, *64*, 1057–1059, (1960).
22. S. V. Mattigod and G. Sposito, "Estimated Association Constants of Some Complexes of Trace Metals with Inorganic Ligands," *Soil Sci. Soc. Am. J.*, *41*, 1092–1097 (1977).
23. X. Feng, J. Liu, G. E. Fryxell, M. Gong, L. Wang, D. E. Kurath, C. S. Ghormley, K. T. Klasson, and K. M. Kemner, *Self-Assembled Mercaptan on Mesoporous Silica (SAMMS) for Mercury Removal and Stabilization* (PNNL-11691), Pacific Northwest National Laboratory, Richland, WA, 1997.

24. D. L. Dugger, J. H. Stanton, B. N. Irby, B. L. McConnel, W. W. Cummings, and R. W. Maatman, "The Exchange of Twenty Metal Ions with Weakly Acidic Silanol Group of Silica Gel," *J. Phy. Chem.*, *68*, 757–760 (1964).
25. G. Sposito, *The Thermodynamics of Soil Solutions*, Oxford University Press, New York, NY, 1981.
26. D. Sparks, *Soil Physical Chemistry*. CRC Press, Boca Raton, FL, 1986.
27. M. Ungarisch and C. Aharoni, "Kinetics of Chemisorption," *J. Chem Soc., Faraday Trans., 77*, 975–985 (1981).

Received by editor September 20, 1998
Revision received November 1998

Request Permission or Order Reprints Instantly!